Dynamic Behavior of a Solid Particle Bed in a Water Pool

Liu, Ping
Department of Applied Quantum Physics and Nuclear Engineering : Graduate Student

Matsumoto, Tatsuya
Institute of Environmental Systems : Associate Professor

Yasunaka, Satoshi
Institute of Environmental Systems : Research Associate

Fukuda, Kenji
Institute of Environmental Systems : Professor

他

出版情報：九州大学工学紀要. 65 (1), pp.53-69, 2005-03. 九州大学大学院工学研究院
バージョン：
権利関係：

Memoirs of the Faculty of Engineering, Kyushu University, Vol. 65, No. 1, March 2005

Dynamic Behavior of a Solid Particle Bed in a Water Pool

by

Ping LIU*, Koji MORITA**, Tatsuya MATSUMOTO***, Satoshi YASUNAKA*,
Kenji FUKUDA**** and Yoshiharu TOBITA*****

(Received December 15, 2004)

Abstract

In order to model the mobility of the postulated disrupted core in a core disruptive accident (CDA) of a liquid metal faster breeder reactor (LMFBR), a series of experiments was performed to simulate the behavior of a solid particle bed in a water pool against pressure transients. Numerical simulations with SIMMER-III code have been performed to verify the validity of SIMMER-III code and to check the influence of the particle jamming model and the particle viscosity model, which are adopted in the code. Comparisons between analytical results and experimental results show that SIMMER-III can well simulate the pressure transients and the particle bed axial height change in the first moment of the nitrogen gas expansion, while giving an earlier second pressure peak value than experiments. The simulation somewhat underestimates the gas volume change in the pressure vessel and the water pool. SIMMER-III results show that the particle jamming model and different assignments of velocity field have obvious influences on the particle volume fraction distribution inside the particle bed.

Keywords: SIMMER-III, Particle bed, Pressure transient, Particle jamming model, Particle viscosity model

1. Introduction

In a core disruptive accident (CDA) of a liquid metal faster breeder reactor (LMFBR), there is a possibility of forming a disrupted core, in which solid particle liquid multi-phase flow is formed due to the existence of mixture of molten fuel, molten structure, refrozen fuel and solid fuel pellets etc. **Figure 1** shows the schematic view of this kind of disrupted core

*Graduate Student, Department of Applied Quantum Physics and Nuclear Engineering
**Associate Professor, Institute of Environmental Systems
***Research Associate, Institute of Environmental Systems
****Professor, Institute of Environmental Systems
*****Japan Nuclear Cycle Development Institute

in a CDA of a LMFBR. It is anticipated that such multi-phase flows might cause the form of a disrupted core with low mobility, in which so-called recriticality due to fuel relocation could be suppressed.

SIMMER-III[1], an advanced safety analysis computer code, has been developed in Japan Nuclear Cycle Development Institute (JNC) to investigate postulated core disruptive accidents in LMFBRs. It is a two-dimensional, three-velocity-field, multiphase, multicomponent, Eulerian, fluid-dynamics code coupled with a space-dependent neutron kinetics model.

It is indispensable for SIMMER-III to simulate the behavior of a solid-phase mixed pool appropriately. Although in SIMMER-III there are models, such as particle jamming model, particle viscosity model, considering the influence of solid particles on multi-phase flow behavior, however, little work has been performed so far on code verification of this behavior.

In this study, a series of experiments was performed to simulate the behavior of solid particle bed in a water pool against pressure transients. **Figure 2** shows the concept of verification experiment.

Numerical simulations by SIMMER-III have also been performed with different model options and different assignments of velocity fields. These simulation results were compared with experimental results as the first step of preliminary code verification.

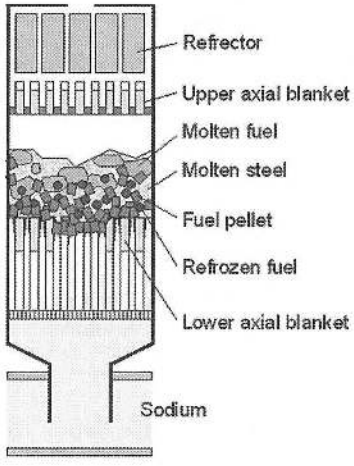

Fig. 1 Schematic view of a disrupted LMFBR core.

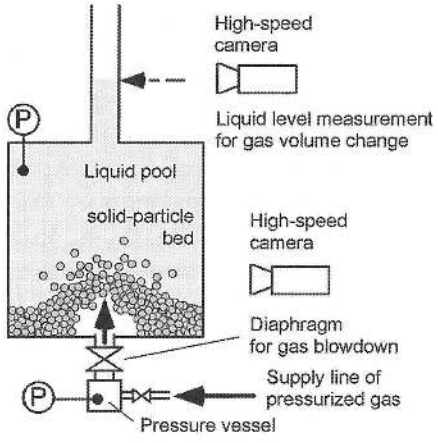

Fig. 2 Schematic view of the verification experiment.

2. Experimental apparatus

A schematic diagram of experimental apparatus is shown in **Fig. 3**. It mainly consists of a cylindrical water pool (inner diameter is 310 mm, height is 1000 mm) made of transparent plexiglass. Steel flanges are used for connections at both the top and the bottom of the cylinder pool. Above the top flange, there is an upper pipe with an inner diameter of 100 mm and height of 500 mm. In the upper pipe, a floater was installed on the water surface to make the water level change recorded by a high-speed camera. Under the bottom flange, there is a pressure vessel of which exit is closed with a rupture disk in the beginning of the experiment. Inside the cylinder pool, a sleeve with an inner diameter of 290 mm and height of 160 mm is used to hold particles. Two plates (total height is 25 mm) are attached at the bottom

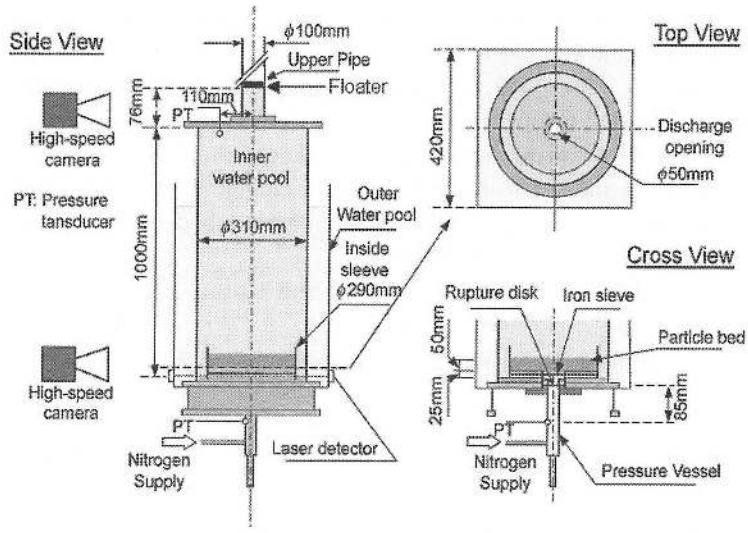

Fig. 3 The Schematic view of experiment apparatus.

of the sleeve. One is for laser beam to pass through for the detection of the injection time of the gas from below. Between the two plates, a metal mesh (with 5.5 mm-apertures) is laid to prevent particles from falling down. The cylindrical water pool is surrounded by a quadrate water pool (420 mm×420 mm×1000 mm) made of transparent plexiglass, in which water is filled to make the visual observation inside the cylinder possible avoiding the convex effect of the cylinder.

The parameters of particles and initial conditions for experiments are shown in **Table 1**. Three kinds of particles, which have different densities and the same diameter of 6mm, were used to form a 50 mm-height particle bed at the bottom of the water pool. For each particle,

Table 1 Experiment parameters.

Particle	AL_2O_3 ρ=3582.8 kg/m^3			Plastic1 ρ=2202.8 kg/m^3			Plastic2 ρ=1008.5 kg/m^3		
Experiment Series	Exp.1	Exp.2	Exp.3	Exp.4	Exp.5	Exp.6	Exp.7	Exp.8	Exp.9
Rupture Disk*	1	2	3	1	2	3	1	2	3
Initial Pressure (MPa)	0.300	0.245	0.199	0.295	0.236	0.198	0.302	0.244	0.202
Initial Particle Volume Fraction	0.64	0.64	0.64	0.61	0.61	0.61	0.65	0.65	0.65
Initial Water Level Height in Upper Pipe, h (mm),	76	127	137	110	171	185	115	115	115
Initial Particle Bed Height, H (mm)	50	50	50	50	50	50	50	50	50
Particle Diameter, D (mm)	6	6	6	6	6	6	6	6	6

* Three kinds of rupture disks (rupture disk 1, rupture disk 2 and rupture disk 3) were used, each of them has a nominal breakage pressure 0.3MPa, 0.25MPa, 0.2MPa, respectively.

three experiment cases with different initial breakage pressures were performed. When the pressure level of the nitrogen gas in the pressure vessel reaches a rupture limit of the disk, the rupture disk breaks and the high-pressure nitrogen gas spurts into the pool driving the particle bed to upward. Two pressure sensors were installed to measure the pressure transients in the pressure vessel and at the top of the water pool, respectively. Two high-speed cameras, both of which can record 400 frames in one second, were used to record the particle bed behavior and the water surface level change in the upper pipe, respectively.

Three reference experiment cases without the particle bed were also performed. The experimental parameters are shown in **Table 2**.

All other parameters were defined under 20°C and 1 atm.

Table 2 Experiment parameters of reference cases.

Reference cases	1	2	3
Initial Pressure (MPa)	0.3053(rupture disk 1)	0.2429(rupture disk 2)	0.1973(rupture disk 3)
Initial Upper Pipe Water Height, h (mm),	119	109	110

3. Experimental results

Exp.1~9 were performed to give results for SIMMER-III code verification. As shown in **Table 1**, most of the experimental cases have two initial parameters different from other cases except Exp.7, Exp.8 and Exp.9, among which initial pressure is the only factor different from each other. Experimental results of these three cases are presented and compared with each other here.

After rupture disk breaks, nitrogen gas ejects from the pressure vessel to the water pool and drives the particle bed upward. **Figure 4** shows the gas volume change in the pressure vessel and the water pool. The data of the gas volume change were obtained from the water surface level change in the upper pipe. **Figure 5** shows the changes of the particle bed height, which were obtained from the recorded particle behavior images. **Figure 6** shows that pressure in the pressure vessel decreased rapidly till the nitrogen expansion ceases and then

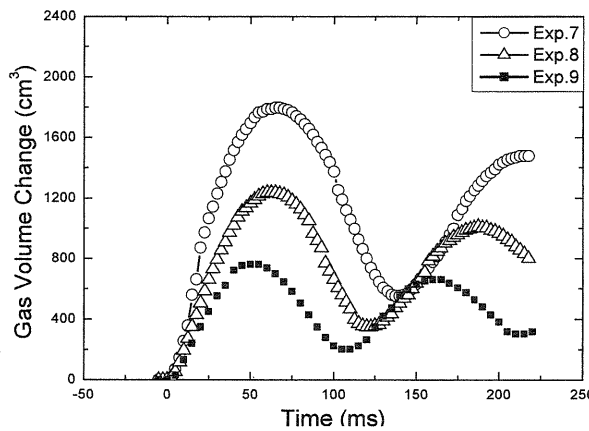

Fig. 4 Gas volume change in the pressure vessel and the water pool.

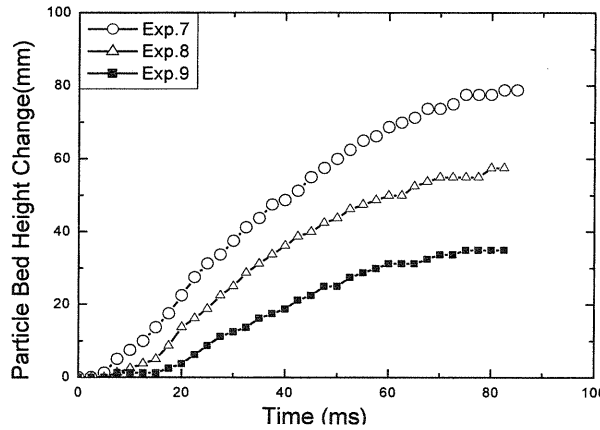

Fig. 5 Particle bed height change.

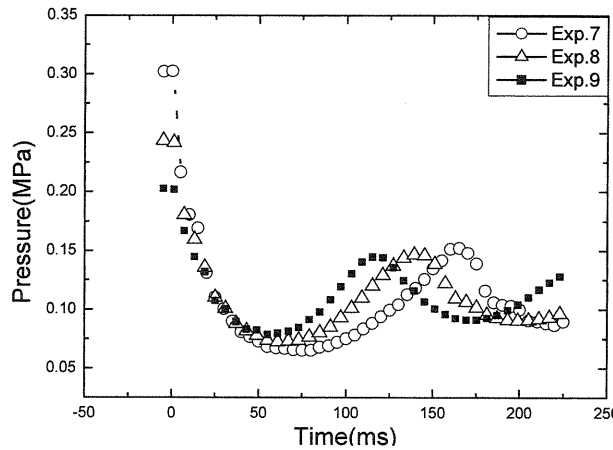

Fig. 6 Pressure transient in the pressure vessel.

increased to its second peak value with the compression of the nitrogen gas. **Figure 7** shows that the pressure at the top of the water pool rapidly increased to its first peak value in about 10ms and then changed corresponding to the transient of the pressure in the pressure vessel.

Table 3 shows the nitrogen expansion time for all experiment series. From the results of Exp.7, Exp.8 and Exp.9, as shown in **Fig. 4** to **Fig. 7**, it is found that the initial pressure has obvious influence on the particle bed movement behavior and the pressure transients. Higher initial pressure causes longer nitrogen expansion time (**Table 3**), bigger gas volume change in the water pool and pressure vessel (**Fig. 4**) and higher particle bed height change (**Fig. 5**). Similarly, longer nitrogen expansion time caused the second peak value of the pressure transients to come later as shown in **Fig. 6** and **Fig. 7**.

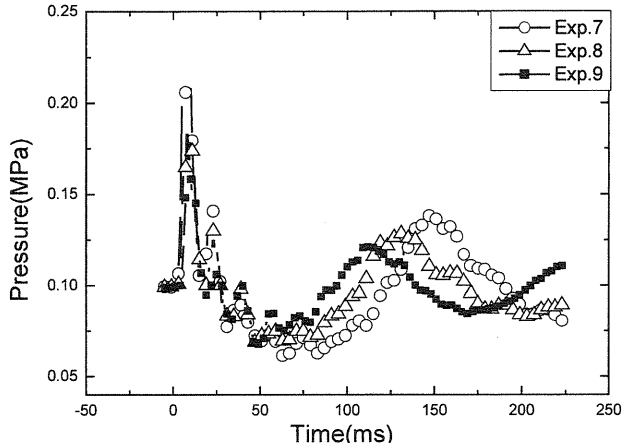

Fig. 7 Pressure transient at the top of the water pool.

Table 3 Nitrogen expansion time for all experiment series.

Particle	AL_2O_3			Plastic1			Plastic2		
Experiment Series	Exp.1	Exp.2	Exp.3	Exp.4	Exp.5	Exp.6	Exp.7	Exp.8	Exp.9
Nitrogen expansion Time (ms)*	62.5	60	55	67.5	65	50	65	60	47.5

* Nitrogen expansion time was chosen in such a way that at this time the gas volume change arrived its first peak value.

4. Numerical simulation by SIMMER-III

SIMMER-III is an advanced safety analysis computer code developed to investigate postulated core disruptive accidents in LMFBR. It is a two dimensional, three-velocity-filed, multiphase, multi-component, Eulerian, fluid-dynamics code[1]. In the current version of SIMMER-III, there are two main models concerned with the influence of the existence of solid particles in pool flow. One is particle viscosity model, which considers the influence of particle volume fraction on the effective liquid viscosity used in momentum conservation equations. The other one is particle jamming model, which defines that solid particles can not enter into but can flow out from a computational cell if in this cell particle volume fraction is over a threshold value.

4.1 Particle viscosity model

In SIMMER-III, the current particle viscosity model uses the following formulation[2]:

$$\mu_c = \mu_L \left\{ \frac{\alpha_L}{\alpha_L + \alpha_P} + \frac{C_{PVIS}\alpha_{MP}\alpha_P}{\alpha_{MP}(\alpha_L + \alpha_P) - \alpha_P} \right\} \tag{1}$$

where μ_c is the effective viscosity of the continuous liquid phase, μ_L is the viscosity of the continuous liquid phase, α_L is the liquid volume fraction, α_P is the particle volume fraction, α_{MP} is the maximum packing fraction of particles. The values of 0.62 and 5.0 are recommend-

ed for α_{MP} and C_{PVIS}, respectively. In the present code, equation (1) is used in the calculation of momentum exchange between the dispersed phase and the continuous liquid phase.

4.2 Particle jamming model

The concept of the particle jamming model is to define a function of volume fraction of particles, which increases exponentially with the increase of particle volume fraction, and add this function directly to the momentum exchange functions in the conservation equations. The following function is used in SIMMER-III[2]:

$$\phi=\max\left\{1.0-\frac{\max(\alpha_P-\alpha_{PJ\max}\beta_{PJ},\,0.0)}{\alpha_{PJ\max}(1.0-\beta_{PJ})},\,0.1\right\}^{C_{PJ}}-1.0 \tag{2}$$

where $\alpha_{PJ\max}$ is the maximum volume fraction of solid particles in a computational cell, β_{PJ} is the maximum volume fraction of dispersed phase in a computational cell, and C_{PJ} is a fitting parameter. In the present code, the values of 0.7, 0.95 and -10.0 are recommended for $\alpha_{PJ\max}$, β_{PJ} and C_{PJ}, respectively.

This function remains 0.0 if $\alpha_P \leq \alpha_{PJ\max}\ \beta_{PJ}$, and increases rapidly when α_P exceeds $\alpha_{PJ\max}\ \beta_{PJ}$.

4.3 Analytical geometry for SIMMER-III simulation

Figure 8 is the schematic view of the analytical geometry used in SIMMER-III simulation. A two-dimensional cylindrical geometry is adopted. In the radial direction 13 cells are defined while the axial direction has 128 cells. For the water pool, there are 83 cells in the axial direction.

All experiment cases use the same computational system except for the upper pipe.

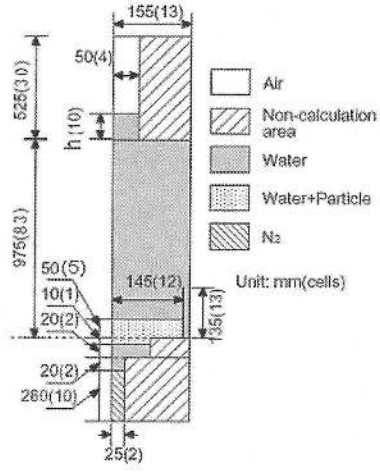

Fig. 8 The analytical geometry for SIMMER-III simulation.

4.4 Results of reference experiment case

Before going to the SIMMER-III simulation of the experiment cases with particle bed, the reference experiments, in which there is no particle bed, were simulated in order to check if there is obvious difference in pressure transients caused by the existence of particles.

Experimental results of the reference experiment case 2 are given here by comparing with SIMMER-III simulation results.

As can be seen from **Fig. 9** to **Fig. 11**, the experimental results of reference case 2 show similar transient trend as that of results of Exp.7 to Exp.9 with particle bed as shown in **Fig. 4**, **Fig. 6** and **Fig. 7**.

In the first nitrogen expansion moment, simulation results of SIMMER-III agree quite well with the experimental results while the second peak pressure value comes earlier than the experiment results. For the gas volume change in the pressure vessel and water pool, **Fig. 11** shows that SIMMER-III underestimates it. Since the data of gas volume change for experiment are obtained from the water surface level change in the upper pipe, one thing needed to be pointed out here is that during the period of experiment, there was some air coming into the pipe area under the floater whose bottom line was the sign of the water surface level, which would have caused some experimental errors and made the gas volume change little bit bigger than real value.

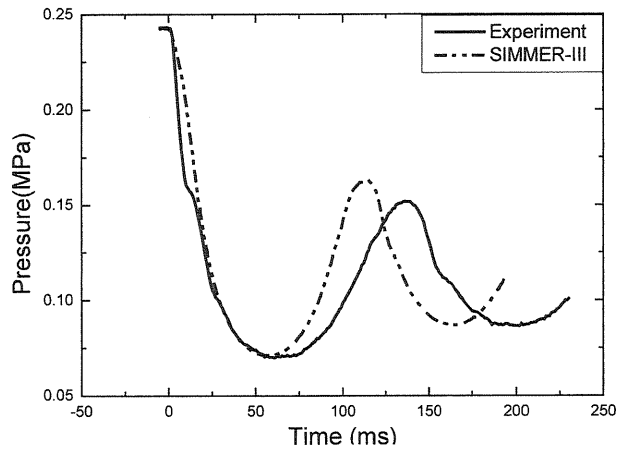

Fig. 9 Pressure transient in the pressure vessel of reference experiment, case 2.

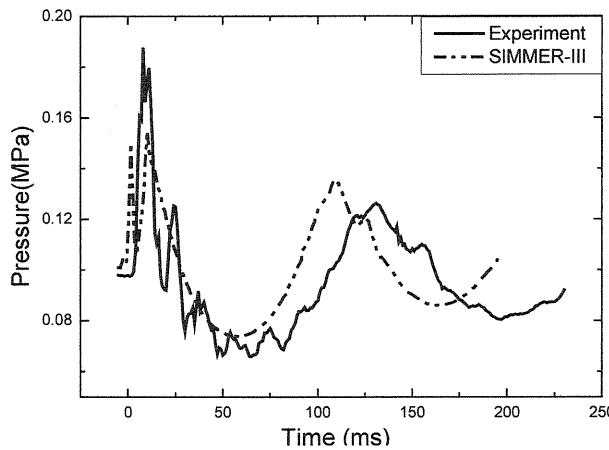

Fig. 10 Pressure transient at the top of the water pool of reference experiment, case 2.

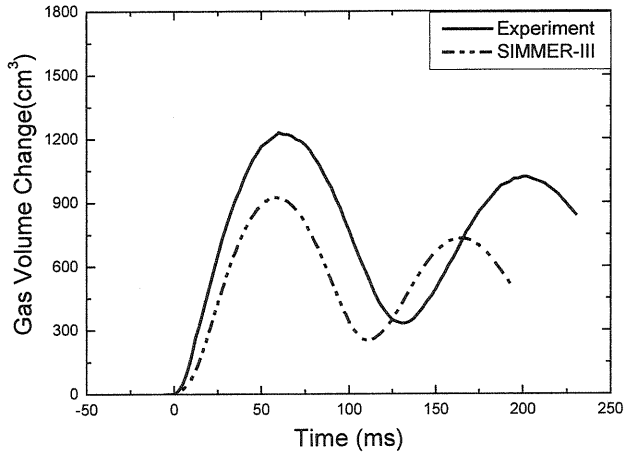

Fig. 11 Gas volume change in the pressure vessel and the water pool of reference experiment, case 2.

4.5 SIMMER-III simulation for experiments with particle bed

In order to check the influence of particle jamming model and particle viscosity model as well as the effect of velocity field assignment, five different cases of SIMMER-III simulation were performed. The definition of these five cases is shown in **Table 4**. In this table, ON and OFF mean that the corresponding model is applied and not applied, respectively; DIFFERENT and SAME mean that water and particles assigned to different velocity field and the same velocity field, respectively.

Table 4 Definition of SIMMER-III simulation cases SIMMER-III simulation cases.

SIMMER-III simulation cases	Particle viscosity model	Particle jamming model	Velocity field assignment of water and particles
Case1	ON	ON	DIFFERENT
Case2	OFF	ON	DIFFERENT
Case3	OFF	OFF	DIFFERENT
Case4	ON	OFF	DIFFERENT
Case5	ON	ON	SAME

4.6 Results and comparison for Exp.2, Exp.5 and Exp.8

Here, all simulation results of experiment cases (Exp.2, Exp.5 and Exp.8) with an initial pressure around 0.25 Mpa are presented and compared with corresponding experimental results.

4.6.1 Pressure transients

Figure 12, **Figure 14** and **Figure 16** show the five cases of SIMMER-III simulation results and experimental results of pressure transients in the pressure vessel for Exp.2, Exp.5 and Exp.8, respectively. All these three figures show that in the first nitrogen expansion moment, the SIMMER-III simulation results agree well with the experimental results but have an earlier second pressure peak than experimental results. This has also been shown in the reference experimental cases.

All five SIMMER-III simulation cases give almost the same results of pressure transient in the pressure vessel.

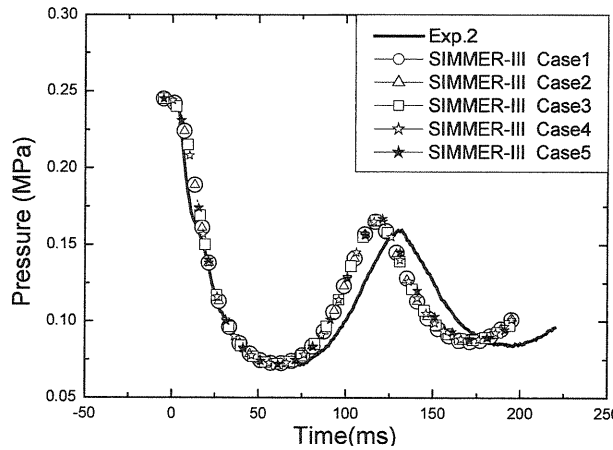

Fig. 12 Pressure transient in the pressure vessel of Exp.2.

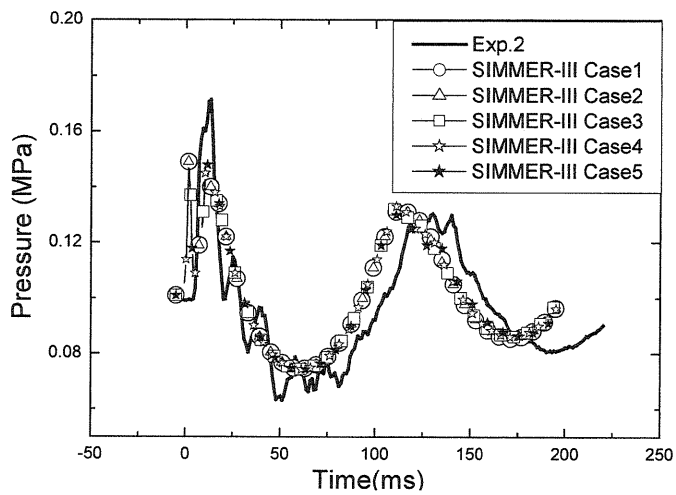

Fig. 13 Pressure transient at the top of the water pool of Exp.2.

Figure 13, **Figure 15** and **Figure 17** show the comparison of SIMMER-III simulation results and experimental results of pressure transients at the top of the water pool for Exp. 2, Exp.5 and Exp.8, respectively. All five SIMMER-III simulation cases also have almost the same pressure transient at the top of the water pool. When compared with the corresponding experiment results, it can be seen that SIMMER-III give a little bit smaller first peak pressure and earlier second peak pressure at the top of the water pool.

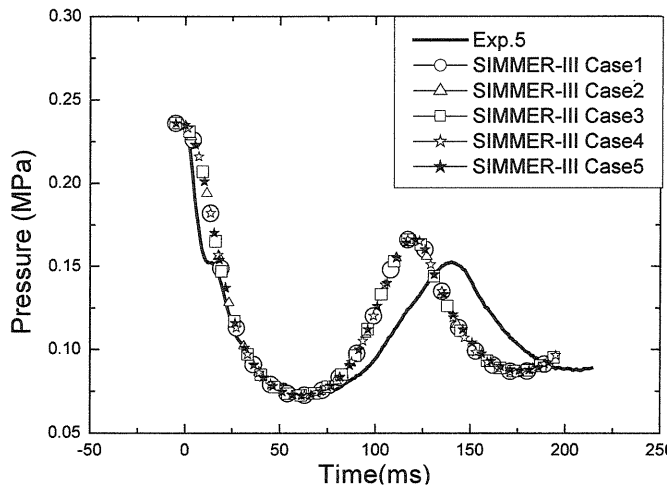

Fig. 14 Pressure transient in the pressure vessel of Exp.5.

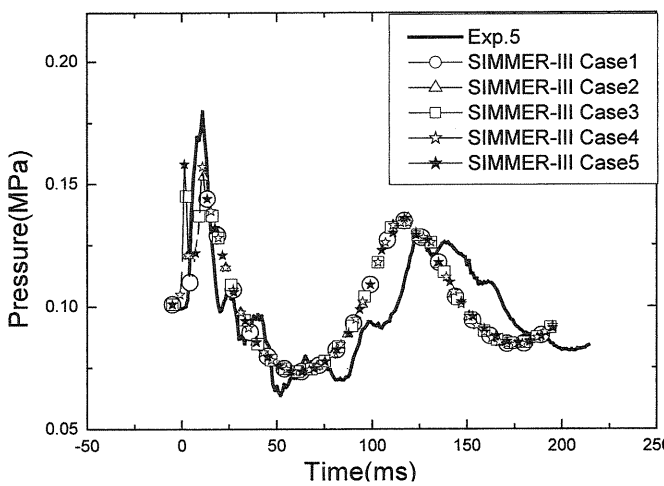

Fig. 15 Pressure transient at the top of the water pool of Exp.5.

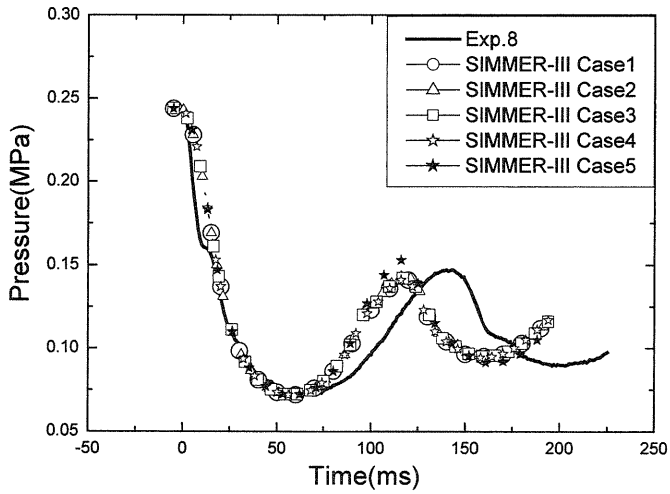

Fig. 16 Pressure transient in the pressure vessel of Exp.8.

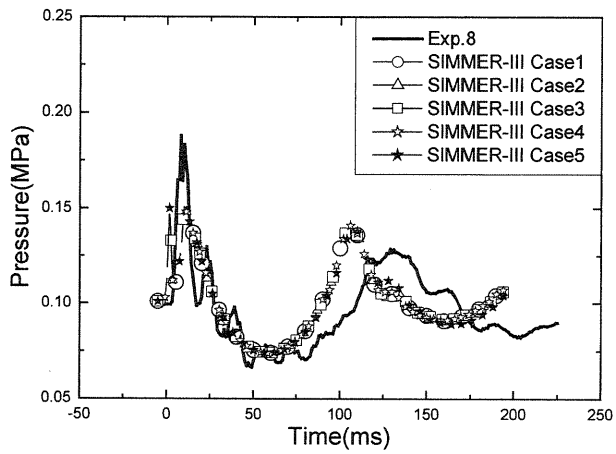

Fig. 17 Pressure transient at the top of the water pool of Exp.8.

4.6.2 Gas volume change

Results for gas volume change in the pressure vessel and water pool are shown in **Fig. 18**, **Fig. 19** and **Fig. 20**. Similar to reference experimental case2, SIMMER-III simulation results underestimate the gas volume change compared with experimental results obtained from the water surface level changes in the upper pipe. Here, it is also needed to notice that experimental error in the measurement of gas volume change as discussed for the reference cases. Considering all SIMMER-III five simulation cases, **Fig. 18**, **Fig. 19** and **Fig. 20** have not shown obvious differences between different model options and velocity field assignments.

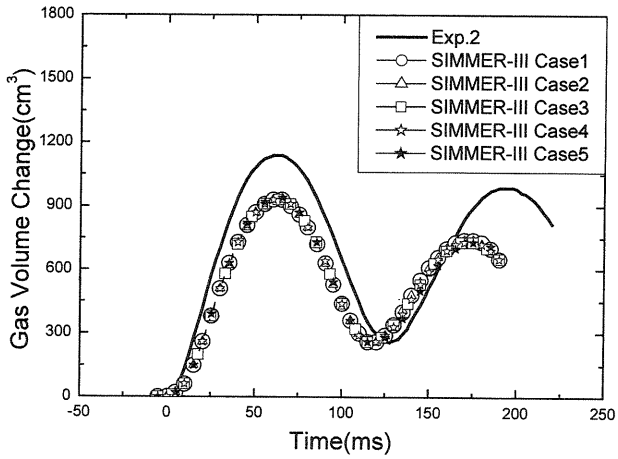

Fig. 18 Gas volume change of Exp.2.

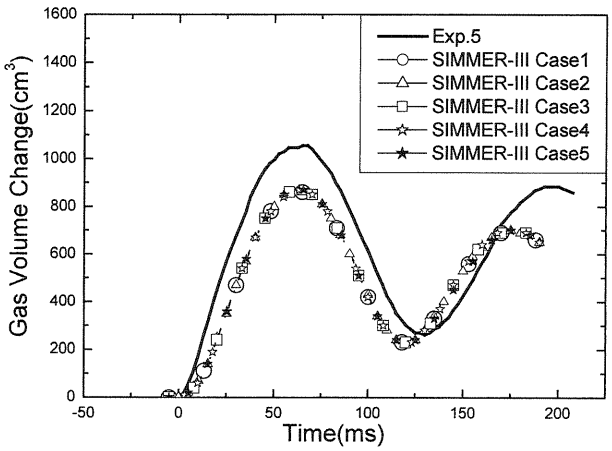

Fig. 19 Gas volume change of Exp.5.

4.6.3 Particle bed height change

Figure 21, **Figure 22**, and **Figure 23** show the particle bed height change in Exp.2, Exp. 5 and Exp.8, respectively. The particle bed height is defined as the particle surface height change in the central axial direction of the water pool. Experimental results shown in these figures were obtained from the images recorded by one of the 400 frames/s high-speed cameras. The SIMMER-III simulation results show the change of the total height of cells in the central axial direction, in which the particle volume fractions were equal or larger than 0.1. Taking mesh cells' sizes used in SIMMER-III simulation into consideration, **Fig. 21** to **Fig. 23** show that in the first 60 ms the SIMMER-III simulation results could represent the particle bed height change measured in Exp.2, Exp.5 and Exp.8. And in the first 60 ms, the results of five SIMMER-III simulation cases do not have significant differences. After the first 60 ms, **Fig. 21** shows that SIMMER-III case1 and case2 have difference from SIMMER-III Case3, Case4 and Case5. However, **Fig. 22** and **Fig. 23** do not show this difference. The

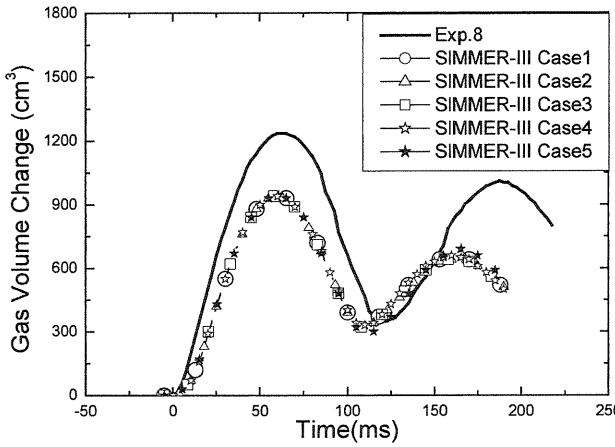

Fig. 20 Gas volume change of Exp.8.

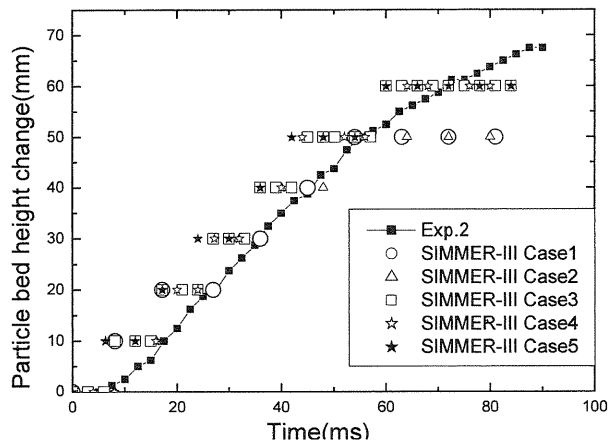

Fig. 21 Particle bed height change of Exp.2.

most obvious difference between Exp.2 and Exp.5, Exp.8 is the difference of particle densities.

4.6.4 SIMMER-III simulation results of particle volume fraction

Although there is no experimental result for particle volume fraction distribution, this part will present some SIMMER-III simulation results of particle volume fraction in cell (1, 16) and cell (6,16) for discussion. Both cells are at the bottom of the water pool while the left boundaries of cell (1,16) and cell (6,16) are 0.0 mm and 62.5 mm away from the center axis, respectively.

Figure 24 and **Figure 26** give the simulation results of particle volume fractions in cell (1,16) of Exp.2 and Exp.8, respectively, while **Fig. 25** and **Fig. 27** give the simulation results of particle volume fractions in cell (6,16) of Exp.2 and Exp.8, respectively.

Figure 24 shows that for cell (1,16) of Exp.2, in the first 125 ms, the SIMMER-III Case1 and Case2 have the same results while SIMMER-III Case3 and Case4 also have the same results, but results of SIMMER-III Case1, Case3 and Case5 are different from each other. This implies that particle jamming model and different velocity field assignments began to

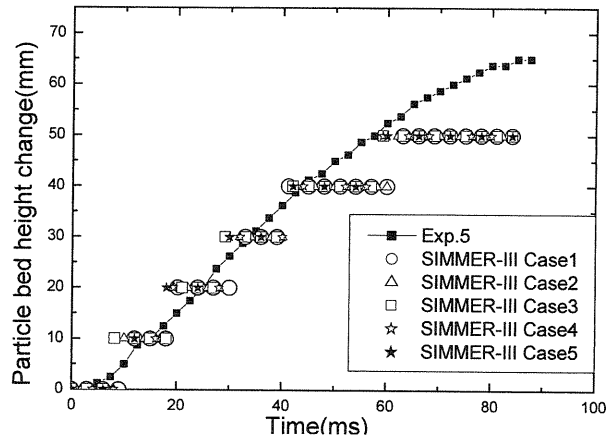

Fig. 22 Particle bed height change of Exp.5.

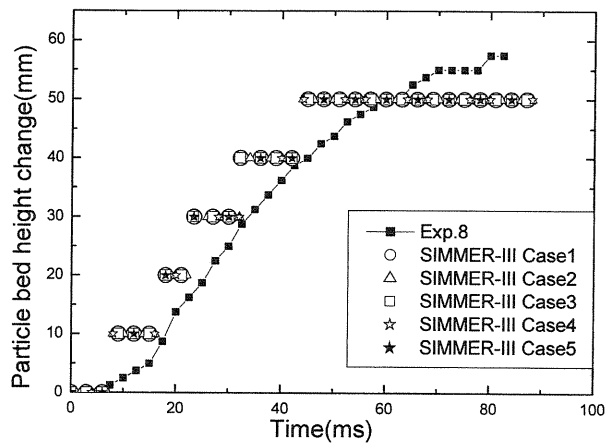

Fig. 23 Particle bed height change of Exp.8.

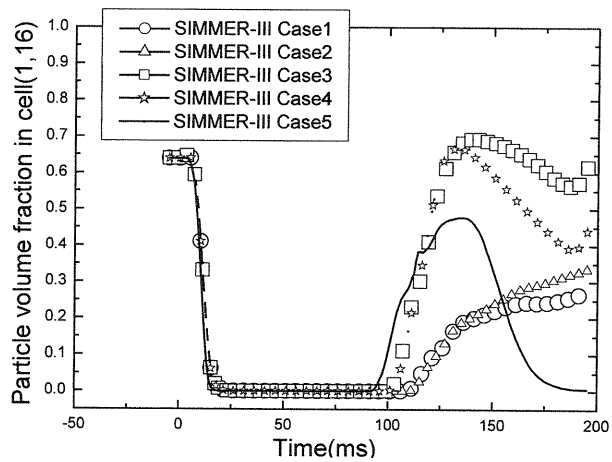

Fig. 24 SIMMER-III simulation results of particle volume fraction in cell (1,16) of Exp.2.

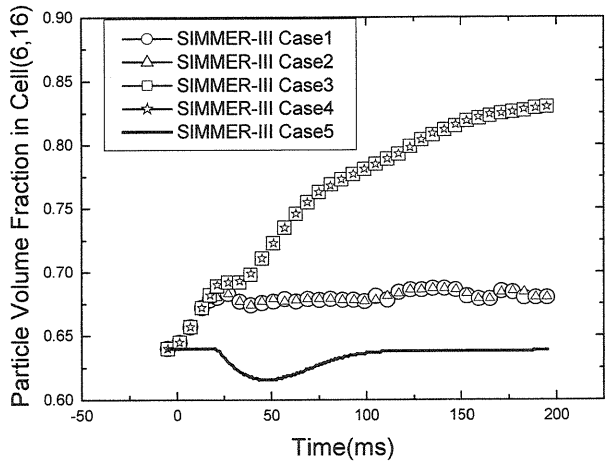

Fig. 25 SIMMER-III simulation results of particle volume fraction in cell (6,16) of Exp.2.

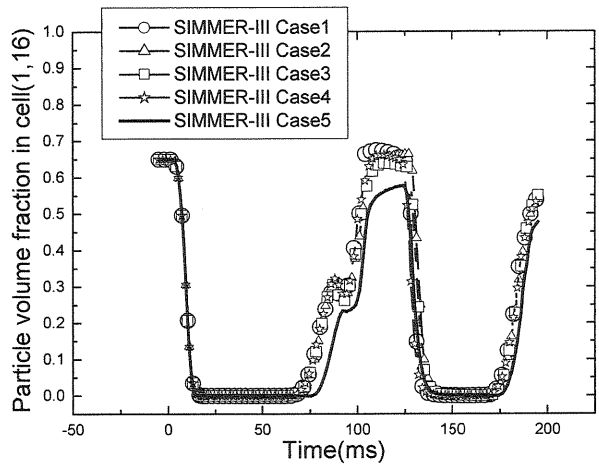

Fig. 26 SIMMER-III simulation results of particle volume fraction in cell (1,16) of Exp.8.

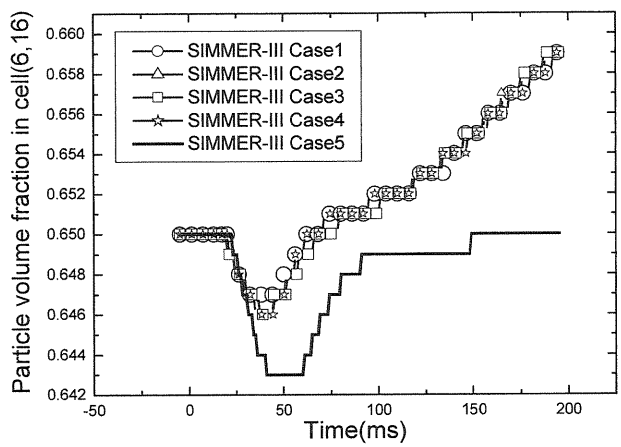

Fig. 27 SIMMER-III simulation results of particle volume fraction in cell (6,16) of Exp.8.

affect the particle volume fraction before 125 ms. After 125 ms, it can be seen that particle viscosity also began to show some influence on the results.

Figure 25 shows that for cell (6,16) of Exp.2, results of SIMMER-III Case1, Case4 and Case5 are different from each other while SIMEMR-III Case1 and Case2 have the same results and SIMMER-III Case3 and Case4 also do. This implies that particle viscosity model does not have obvious influence, while the particle jamming model has important influence on the particle volume fraction. Velocity field assignments also affect the particle volume fraction.

However, for Exp.8, **Fig. 26** and **Fig. 27** have not show the same obvious differences caused by particle jamming model as explained above. The most significant differences between Exp.2 and Exp.8 lie in the particle densities. Combining the above discussion of the influence of particle jamming model on the particle bed height change, it may be possible that solid particle density would also affect the influence of particle jamming model on particle phase distribution. For the pool flow condition, the effect of particle density on other models needs to be investigated further.

5. Conclusion and future work

In this study, a series of experiments was performed to simulate the behavior of solid particle bed in a water pool against pressure transients. The experimental results show that the higher initial pressure results in the longer nitrogen expansion time, the larger gas volume change in the water pool as well as in the pressure vessel and the higher particle bed height change.

The comparison between SIMMER-III simulation results and experimental results shows that SIMMER-III can well simulate the pressure transients and particle bed height change in the first moment of nitrogen gas expansion while giving a little bit earlier second pressure peak value than experimental results and underestimating the gas volume change in the pressure vessel and water pool. Particle jamming model and particle viscosity model with recommended parameters did not show obvious influence on the pressure transients, gas volume change and the particle bed axial height change, while results of SIMMER-III simulation of different model options show that different assignments of velocity field have influences on the particle volume fraction distribution. In experimental cases with large particle density the effect of particle jamming model on particle phase distribution inside particle bed is obvious.

To improve the SIMMER-III code, further investigation on the influence of particle density is needed. For the models of particle viscosity and particle jamming, the effect of particle diameter would be considered. Therefore, a new series of experiments will be performed to verify the code against the dynamic behavior of the solid-particle bed with variety of particle size.

References

1) H. Yamano et al, SIMMER-III: A Computer Program for LMFR Core Disruptive Accident Analysis −Version 3. A Model Summary and Program Description−. O-arai Engineering Center, Japan Nuclear Cycle Development Institute, JNC TN9400 2003-071, 2003.

2) Y. Tobita, Momentum Exchange Function Model in SIMMER-III (Research Document), O-arai Engineering Center, Japan Nuclear Cycle Development Institute, to be published.